Electronic Supplementary Material (ESI) for Soft Matter.

Supporting Information:

Compact Polar Moieties Induce Lipid-Water Systems to Form Discontinuous Reverse Micellar Phase

Manoj Kumar,[a]Naganath G. Patil,[b]Chandan Kumar Choudhury,[c]SudipRoy,[c]Ashootosh V. Ambade[b] and Guruswamy Kumaraswamy*[a].

a. *Complex Fluids and Polymer Engineering, Polymer Science and Engineering Division, CSIR-National Chemical Laboratory, Dr. Homi Bhabha Road, Pune 411008, Maharashtra, India. Phone: +91-20-2590-2182; Fax: +91-20-2590-2618, E-mail: g.kumaraswamy@ncl.res.in*

b. *Polymer Science and Engineering Division, CSIR-National Chemical Laboratory, Dr. Homi Bhabha Road, Pune 411008, Maharashtra, India.*

c. *Physical Chemistry Division, CSIR-National Chemical Laboratory, Dr. Homi Bhabha Road, Pune 411008, Maharashtra, India.*

Table of contents

Section I.
[Schemes: Sm1-Sm4; Figures: S1-S8]

A) Material and synthesis:

Scheme Sm1: Synthesis of PAMAM Dendron **(**PAMAM G1 Amine, PAMAM G2 Amine, PAMAM G3 amine, PAMAM G4 amine)
Scheme Sm2: Synthesis of PAMAM-G4 PEG Dendron **(**PEG-PAMAM G4)

Scheme Sm3: Synthesis of monomer (Boc-AEMA)

Scheme Sm4: Synthesis of Linear Polymers (Poly-AEMA)

B) Characterisation:

Figure S1: ^{1}H NMR spectrum of PAMAM G4 PEG

Figure S2: GPC Analysis for poly-AEMA

Figure S3: ^{1}H NMR spectrum of N-Bocethylenediamine

Figure S4: ^{1}H NMR spectrum of Boc-AEMA

Figure S5:^{1}H NMR spectrum of L3-Boc

Figure S6: ^{1}H NMR spectrum of L3

Figure S7: ^{1}H NMR spectrum of L4-Boc

Figure S8: ^{1}H NMR spectrum of L4

Section II.
[Figures: S9-S19; Tables: ST1-ST3]

C) Experimental Section:

Figure S9: Control experiment comparing pure GMO (purity > 99%) and commercial GMO (Rylo)
Figure S10: Optical images for different liquid crystalline mesophases between crossed polarizers
Figure S11: SAXS diffraction peaks for the GMO/water (80/20) w/w system in the presence of 6 wt. % G2, G3, and G4 are plotted as the peak spacing q_{hkl} *versus* $(h^2+k^2+l^2)^{1/2}$.
Figure S12: SAXS data for GMO/water**: (a)** 85/15 w/w; **(b)** 80/20 w/w; **(c)** 75/25 w/w containing Φ = 0, 2, 4 and 6 wt%, of G2 PAMAM dendron
Figure S13: SAXS data for GMO/water**: (a)** and **(a*)** 80/20 w/w; **(b)** 85/15 w/w; **(c)** 75/25 w/w containing G3 PAMAM dendron and L3 (linear analog).
Figure S14: SAXS data for GMO/water**: (a)** 85/15 w/w; **(b)** 75/25 w/w containing Φ= 0, 2, 4 and 6 wt%, of G4 PAMAM dendron
Figure S15: Plot shows that Pn3m (in excess of water) phase with 50/50 (GMO/Water) system transforms into Fd3m phase with G4 PAMAM
Figure S16: Lattice parameter for Fd3m phase in GMO/water/G4 PAMAM (f_w = 4%) system, as a function of water content.

Figure S17: Kinetics of phase transformation: we observe structural changes for the 80:20:4 GMO/water/G4 systems as a function of equilibration time.
Figure S18: GMO/Water/G4-PEG-PAMAM system formed coexisting-Pn3m phase in 80:20:6 compositions (preferably Pn3m).
Figure S19: a) Represents the chemical structure for the POSS molecule b) Represents the chemical structure for branched PEI.
Table ST1: Creep viscosity measurement for GMO/water (80/20) system with G4 and L4 as a function of Φ.
Table ST2: Lattice parameter characterizing L_{α}, H_{II} and Fd3m phases for GMO/water (85/15) with G2, G3 and G4 PAMAM dendrons.
Table ST3: Lattice parameter characterizing Ia3d, H_{II} and Fd3m phases for GMO/water (75/25) with G2, G3 and G4 PAMAM dendrons.

Section III

[Figures: S20-S24; Tables: ST4-ST6]

D) Computational Details:

Figure S20: Structure of modified LPAMAM and GMO.
Figure S21: Representation of self-assembled GMO and water molecules.
Figure S22: Shows the collapsed state of G4 and extended state of L-PAMAM molecules.
Figure S23: The radial distribution of N, O atoms with other N, O atoms and the radial distribution of N atoms around the O atoms.
Figure S24: The volume normalized distance between the head group oxygen atom of GMO and the N and O atoms of the polymer, G4 and L4.
Table ST4: Force Field Parameters for G4.
Table ST5: Force Field Parameters for L-PAMAM.
Table ST6: Lennard Jones parameter for the different atom types.

Section I

A) Materials and synthesis:

Glycerol monooleate (GMO), commercially known as Rylo MG 20 pharma was received as a generous gift from Danisco Corporation (India). GMO is an amphiphilic molecule with a reported HLB value of 3.9. [1] Rylo contains ≥ 95% GMO, and has an acid value of 2.4. NMR characterisation confirms the presence of GMO as major component in the sample.[2]We estimate, by titration, that there is 1.3% free fatty acid in Rylo.

Synthesis of dendrons:

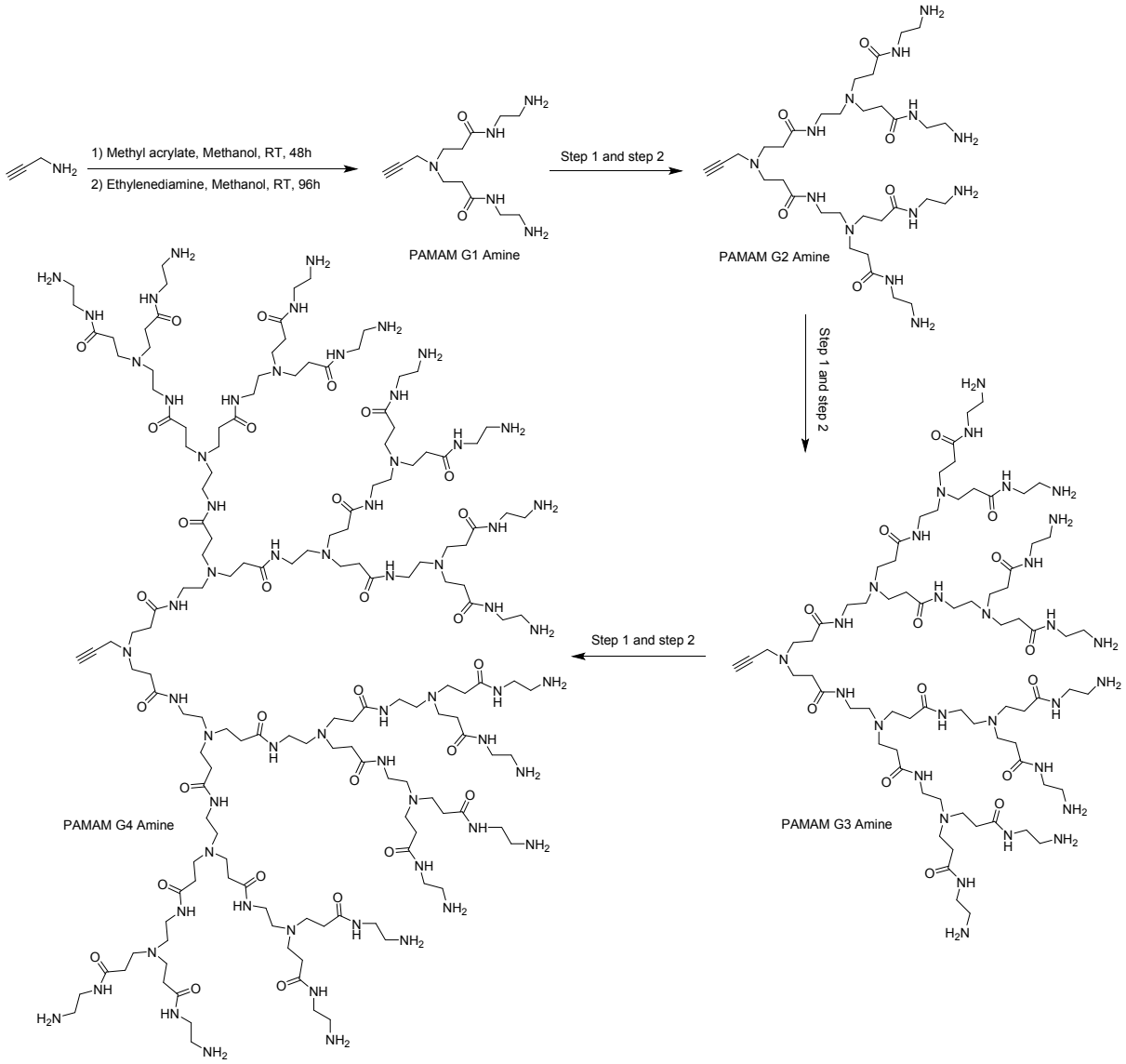

Scheme Sm1: Synthesis of PAMAM dendron with peripheral amines from G1 to G4 generation according to reported procedure.[3]

PAMAM G1 Amine: Pale yellow oil, yield 99.2%,^{1}H NMR (200 MHz, $CDCl_3$): δ (ppm) 2.21(1H, -C*H*CCH$_2$-), 2.36(4H, -C*H*$_2$CONH-), 2.85(8H, RNC*H*$_2$-, -C*H*$_2$NH$_2$), 3.25(4H, -HNC*H*$_2$-), 3.45(2H, -CHCC*H*$_2$-), 7.31(2H –CON*H*-), $C_{13}H_{25}N_5O_2$, Mol. Wt. Calcd. $[M]^+$ 283.38, MALDI-TOF (M+H, M+Na): (284.3, 306.37).

PAMAM G2 Amine: Pale yellow oil, yield 98%, ^{1}H NMR (200 MHz, $CDCl_3$): δ (ppm) 2.22(1H, -C*H*CCH$_2$-), 2.34(12H, -C*H*$_2$CONH-), 2.52(4H, -C*H*$_2$NR$_2$-), 2.72-2.82(20H, RNC*H*$_2$-, -C*H*$_2$NH$_2$), 3.27(12H, -HNC*H*$_2$-), 3.45(2H, -CHCC*H*$_2$-), 7.65-7.92(6H CON*H*-), $C_{33}H_{65}N_{13}O_6$,Mol. Wt. Calcd. $[M]^+$ 739.97, MALDI-TOF found (M+H, M+Na): (741.12, 763.21).

PAMAM G3 amine: Pale yellow oil, Yield 98%,^{1}H NMR (200 MHz, $CDCl_3$): δ (ppm) 2.26 (1H, -C*H*CCH$_2$-), 2.36(28H, -C*H*$_2$CONH-), 2.52(12H, -C*H*$_2$NR$_2$-), 2.74-2.84(44H, RNC*H*$_2$-, -C*H*$_2$NH$_2$), 3.27(28H, -HNC*H*$_2$-), 3.45(2H, -CHCC*H*$_2$-), 7.75-8.02(14H CON*H*-). $C_{73}H_{145}N_{29}O_{14}$, Mol. Wt. Calcd. $[M]^+$ 1653.15, MALDI-TOF (M+H, M+Na): (1654.27, 1676.29).

PAMAM G4 amine: Pale yellow sticky solid, Yield 95%,^{1}H NMR (200 MHz, DMSO-d_6): δ (ppm) 2.15(61H, -C*H*CCH$_2$-, -C*H*$_2$CONH-), 2.38(28H, -C*H*$_2$NR$_2$-), 2.54(32H, RNC*H*$_2$-), 2.63(32H, -C*H*$_2$NH$_2$), 3.04(60H, -HNC*H*$_2$-), 3.35(2H, -CHCC*H*$_2$-), 7.92-7.97(30H CON*H*-). $C_{153}H_{305}N_{61}O_{30,}$ Mol. Wt. Calcd. $[M]^+$ 3479.52, MALDI-TOF (M+H, M+Na): (3480.43, 3503.51).

PEG-PAMAM G4:

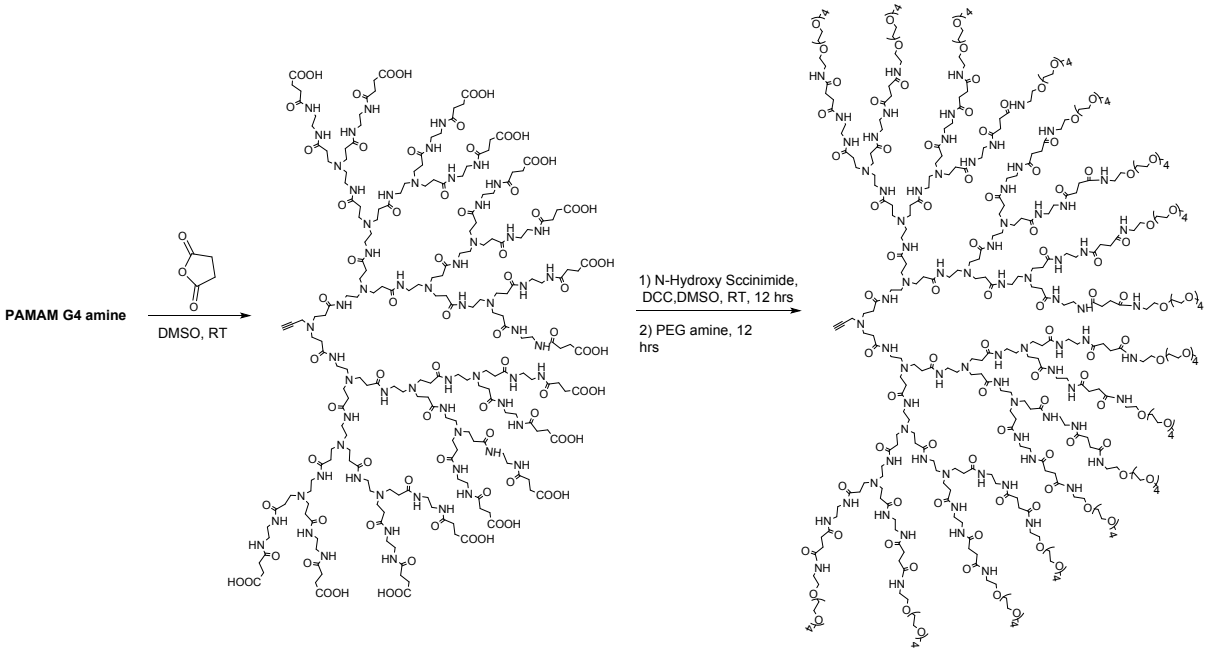

Scheme Sm2: Synthesis of PAMAM-G4 PEG dendron

PAMAM G4 amine (1 g, 0.29 mmol) was dissolved in 15 mL of DMSO in round bottom flask. To this solution, 10 mL of DMSO containing succinic anhydride (1.024 g, 10.24 mmol) was added under vigorous stirring and stirred for 24h. The reaction mixture was precipitated in large amount of acetone, re-precipitated by dissolving in DMSO. Finally, precipitate was allowed to settle down and acetone removed by decantation, again fresh acetone was added and stirred. This procedure was repeated till fine powder of PAMAM-G4-COOH was obtained. The product was dried in vacuum oven at room temperature for 48 h to get desired compound. Yield 1.46 g, 99%. ^{1}H NMR (200 MHz, DMSO-d_6): δ (ppm)2.16(57H, -C*H*CCH$_2$-, -C*H*$_2$CONH-), 2.26(32H, -COC*H*$_2$CH$_2$COOH), 2.37-2.39(60H -COCH$_2$C*H*$_2$COOH, -C*H*$_2$NR$_2$-), 2.63(56H, RNC*H*$_2$), 3.03(92H, -HNC*H*$_2$-, -HNC*H*$_2$C*H*$_2$NH-), 3.34(2H, -CHCC*H*$_2$-), 7.81-7.90(44H, -CON*H*-). PAMAM-G4-COOH (0.5g 0.0984 mmol) and N- hydroxysuccinimide (0.543 g, 4.72 mmol) were dissolved in 5.0 mL of dry DMSO, and then (3.208 g, 15.549 mmol) of *N*,*N*-dicyclohexylcarbodiimide (DCC) was added. The reaction solution was stirred at room temperature overnight and then filtered to remove the white precipitate of *N*,*N*-dicyclohexylurea (DCU). Amine-functionalized pentaethylene glycol (PEG) (0.790 g, 3.149 mmol) was added and stirred at room temperature overnight. Once the reaction was complete, the traces of DCU were removed by filtration. The crude product was precipitated in diethyl ether, dried, re-dissolved in dichloromethane, precipitated in diethyl ether and dried under vacuum. ^{1}H NMR (200 MHz, $CDCl_3$): δ (ppm)) 2.30-2.80(-C*H*CCH$_2$-, -C*H*$_2$CONH-, -COC*H*$_2$C*H*$_2$CONH-, -C*H*$_2$NR$_2$-, RNC*H*$_2$), 3.0-3.13(-HNC*H*$_2$-, -HNC*H*$_2$C*H*$_2$NH-), 3.14-3.22 (-CONH-C*H*$_2$) 3.23(-OC*H*$_3$) 3.35-3.60(OC*H*$_2$) 7.85-8.70(-CON*H*-).

Synthesis of linear polymer

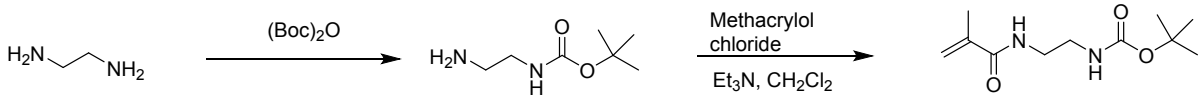

SchemeSm3. Synthesis of Monomer

a) Synthesis of N-Boc ethylenediamine:

In 500 ml two neck round bottom flask ethylenediamine (18.2g, 302 mmol) and 250 ml dichloromethane was added and cooled to 0 ^{0}C. In another flask Di-*tert*-butyl dicarbonate (10g, 45.8 mmol) was dissolved in 50 ml dichloromethane and drop wise added to above solution. After completion of addition the reaction mixture was stirred for 12h at room temperature. The precipitate was filtered and washed with dichloromethane. The filtrates were collected and solvents were evaporated, re-dissolved in ethyl acetate and washed with brine (100 ml , 3 times) and 100 ml water. The organic layer was dried over sodium sulphate filtered and evaporated to get N-Boc ethylenediamine. Yield 4.2g, 57% as colourless oil. ^{1}H NMR (200 MHz, $CDCl_3$): δ (ppm) 4.96 (bs, 1H, -N*H*-), 3.14 (q, 2H, CH_2-C*H*$_2$-NH), 2.77 (t, 2H, C*H*$_2$-CH_2-NH), 1.43 (s, 9H, -C(C*H*$_3$)$_3$), 1.37 (bs 2H, N*H*$_2$).

b) Synthesis of N-2-[(tert-butoxycarbonyl)amino] ethyl methacrylamide (Boc-AEMA):

To N-Boc ethylenediamine (4.05g, 25.3 mmol) in 50 ml dry dichloromethane triethyl amine (4.25 ml, 30.3 mmol) was added. The reaction mixture was cooled in ice bath to this methacryloyl chloride (2.64g, 25.3 mmol) in 10 ml dichloromethane was added dropwise with stirring. After complete addition the reaction mixture was stirred to room temperature overnight then the reaction mixture was washed with water (100 ml, 3 times) and brine solution. The organic layer was dried over

sodium sulphate, filtered and evaporated. Purification was done by silica gel column chromatography with ethyl acetate: pet ether (20:80) as eluent to get pure product as white solid which further purified by recrystallization in ethanol. Yield 4.8g, 83% ^{1}H NMR (200 MHz, $CDCl_3$): δ (ppm), 6.81 (bs, 1H,-N*H*), 5.75 (s, 1H, -N*H*), 5.32 (t, 1H, C*H*$_2$=C), 5.06 (bs, 1H, C*H*$_2$=C), 3.48-3.24 (m 4H, -C*H*$_2$-C*H*$_2$-NH), 1.95 (s, 3H, CH_2=C(C*H*$_3$)), 1.42 (s, 9H, -C(C*H*$_3$)$_3$).

c) Polymerization:

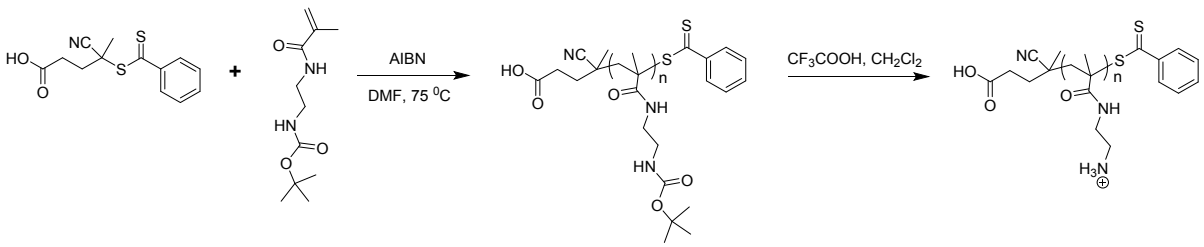

Scheme Sm4: Synthesis of monomers and Linear Polymers (Poly-AEMA)

Into a Schlenk tube Boc-AEMA was dissolved in DMF (1M conc.) and purged with nitrogen for 30 min with continuous stirring. 4-cyano-4(phenylcarbonothioylthio)pentanoic acid (CTA) and AIBN were introduced under nitrogen atmosphere, reaction mixture was stirred get homogenous mixture and degassed by three freeze-pump-thaw cycles. Then reaction mixture was inserted into pre-heated oil bath at 75 ^{0}C and stirred for 12h. The reaction was quenched by cooling in liquid nitrogen and reaction mixture was precipitated in ethyl acetate:pet ether (40:60). Precipitation procedure was repeated several times from solution in dichloromethane for complete removal of monomer. Poly-Boc-AEMA was obtained as pink solid. Deprotection of Boc group was carried out by dissolving the polymer into 10 mL mixture of trifluroacetic acid:dichloromethane (1:1) and stirred at room temperature overnight. The solvents were removed under vacuum and rinsed with diethyl ether three times. The polymer obtained was dried under vacuum. Removal of Boc group was confirmed from ^{1}H NMR spectrum.

Poly-(Boc-AEMA) (L-Boc): ^{1}H NMR (200 MHz, $CDCl_3$): δ (ppm), 7.30-7.80, 6.40-7.20, 5.20-6.10, 3.29, 2.52, 1.6-2.4, 1.44, 0.7-1.2.

Poly-AEMA (L): ^{1}H NMR (200 MHz, DMSO-d_6): δ (ppm), 7.3-8.25, 3.3-3.60, 2.85, 2.10-2.4, 1.4-2.0, 0.6-1.35

B) Characterisation:

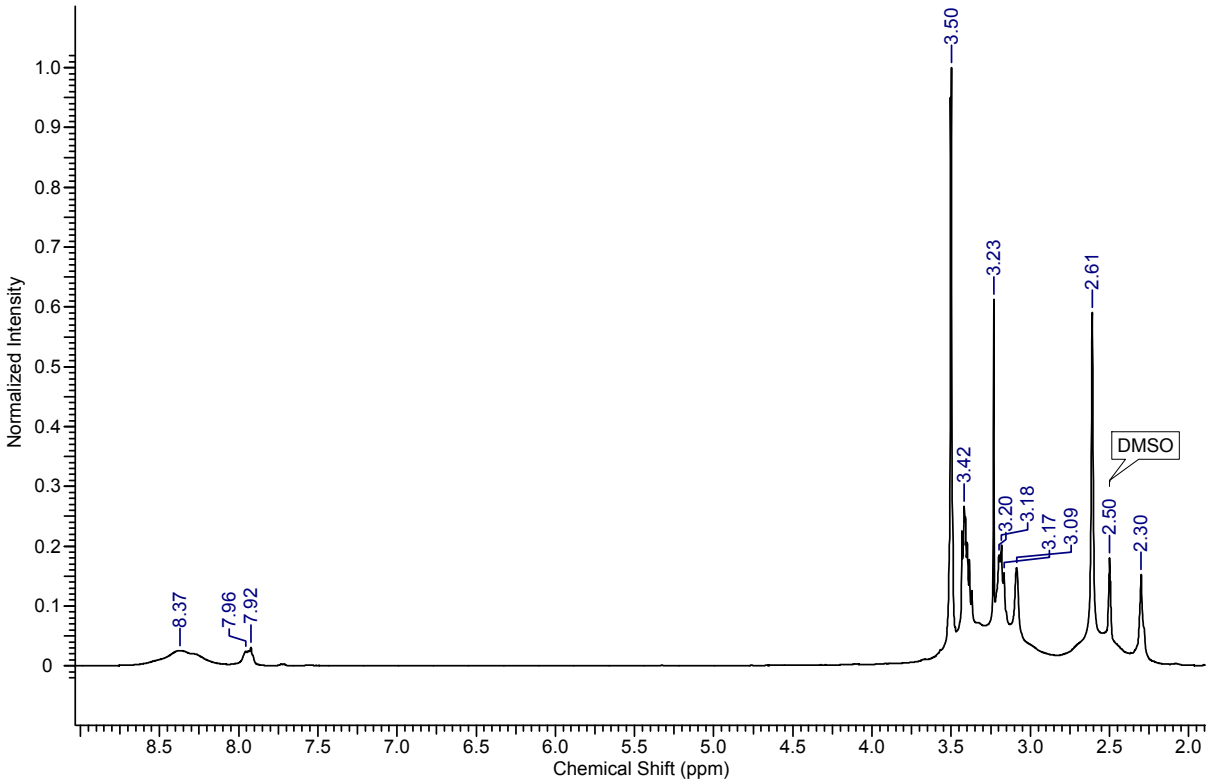

Figure S1. 400 MHz ^{1}H NMR spectrum of PAMAM G4 PEG in DMSO-d_6

GPC Analysis:

Poly-Boc-AEMA$_{10}$ (L3-Boc): GPC M_n = 1400, PDI= 1.20

Poly-Boc-AEMA$_{20}$ (L4-Boc): GPC M_n = 2100, PDI= 1.28

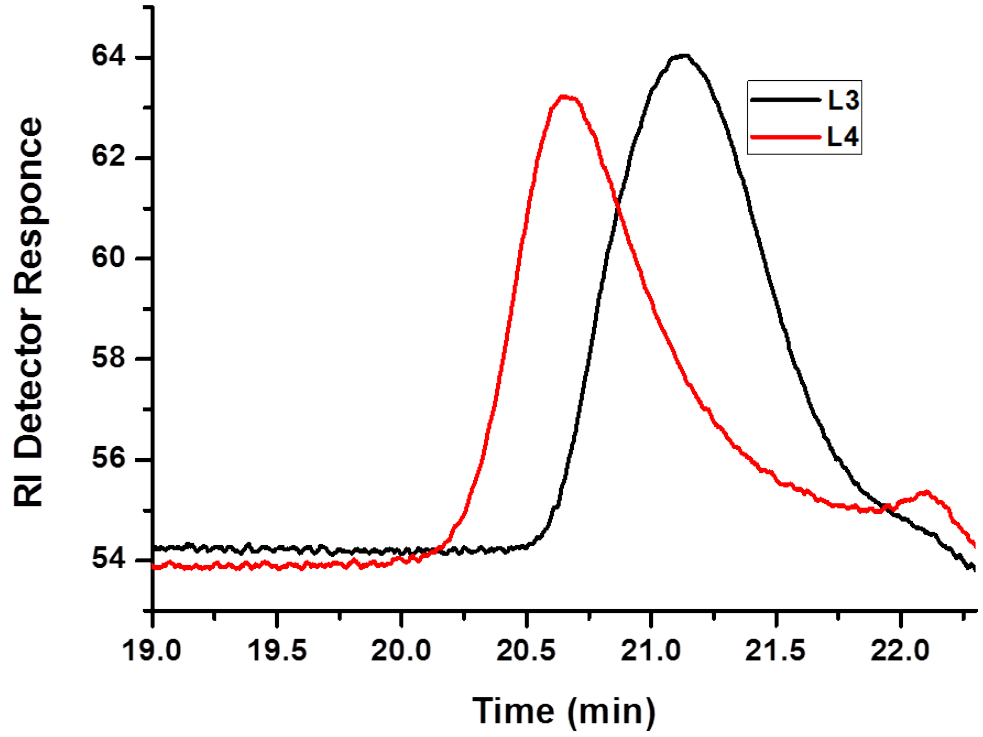

Figure S2: GPC Spectra of L3 and L4 were done using THF as eluent against polystyrene standards.

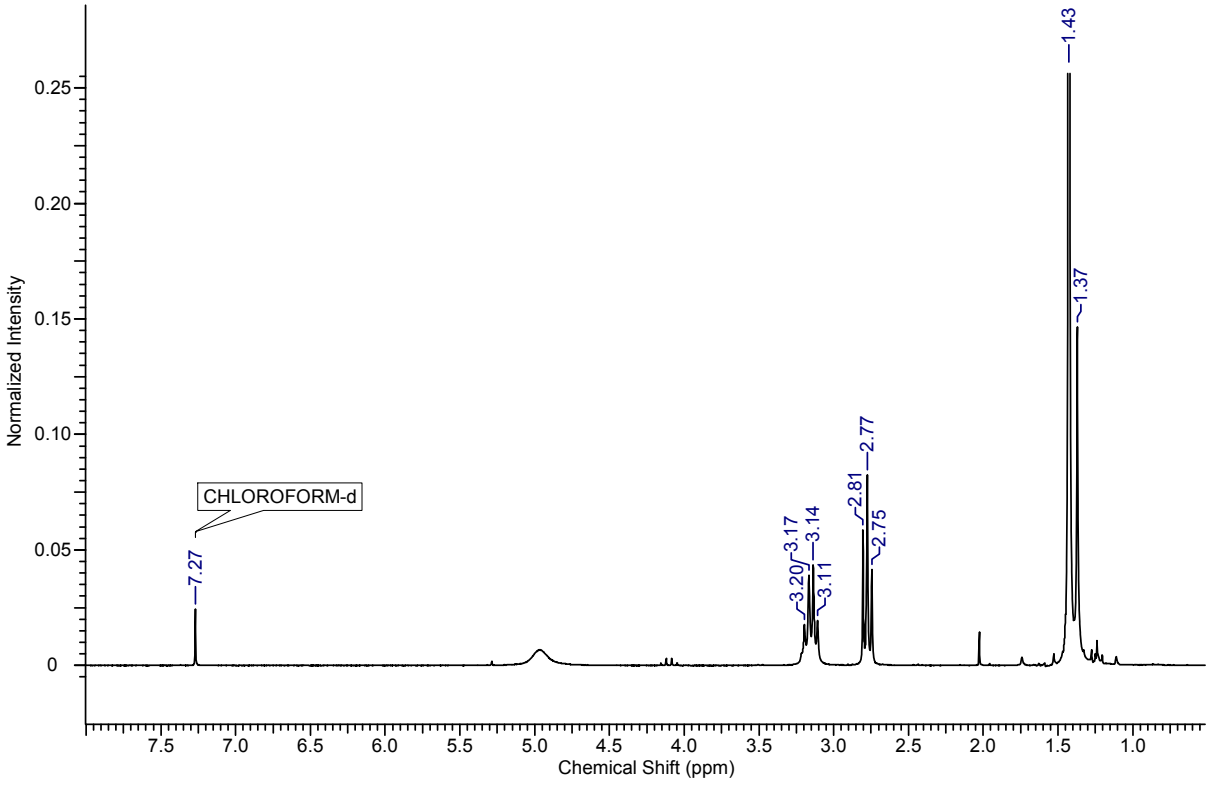

Figure S3. 200 MHz ^{1}H NMR spectrum of N-Boc ethylenediamine in $CDCl_3$

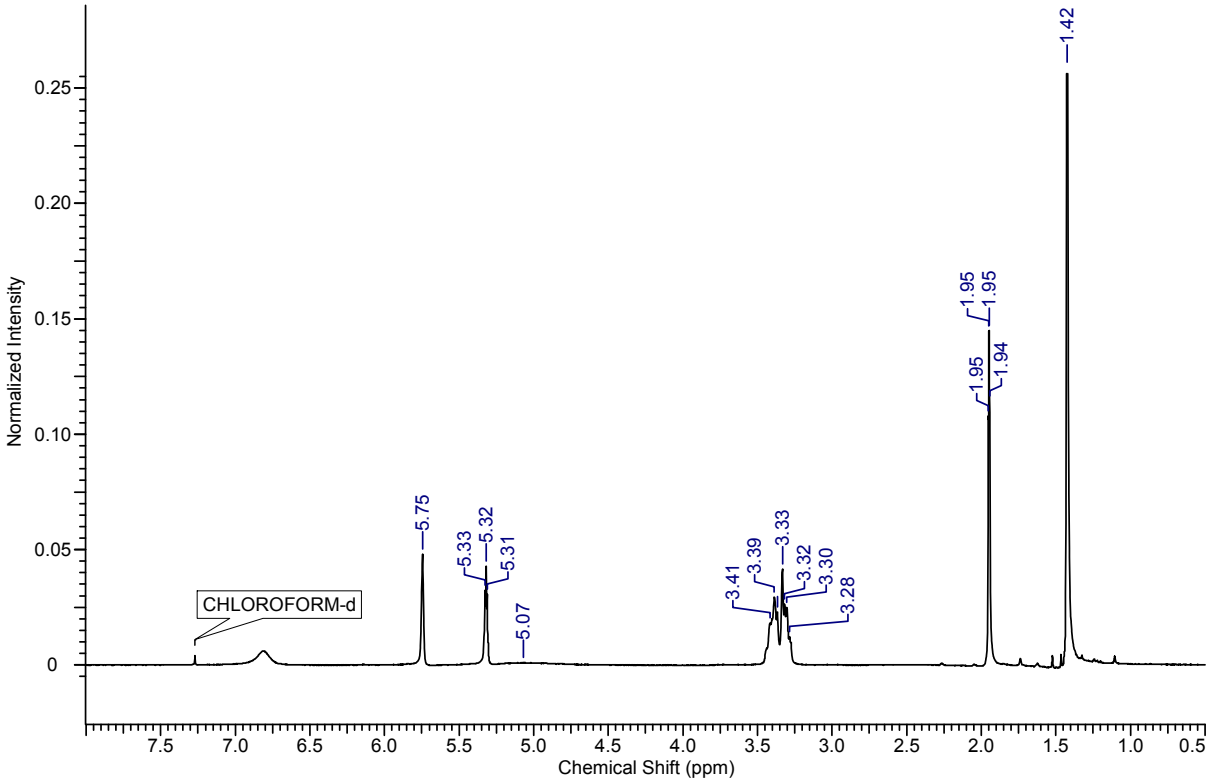

Figure S4. 200 MHz ^{1}H NMR spectrum of Boc-AEMA in $CDCl_3$

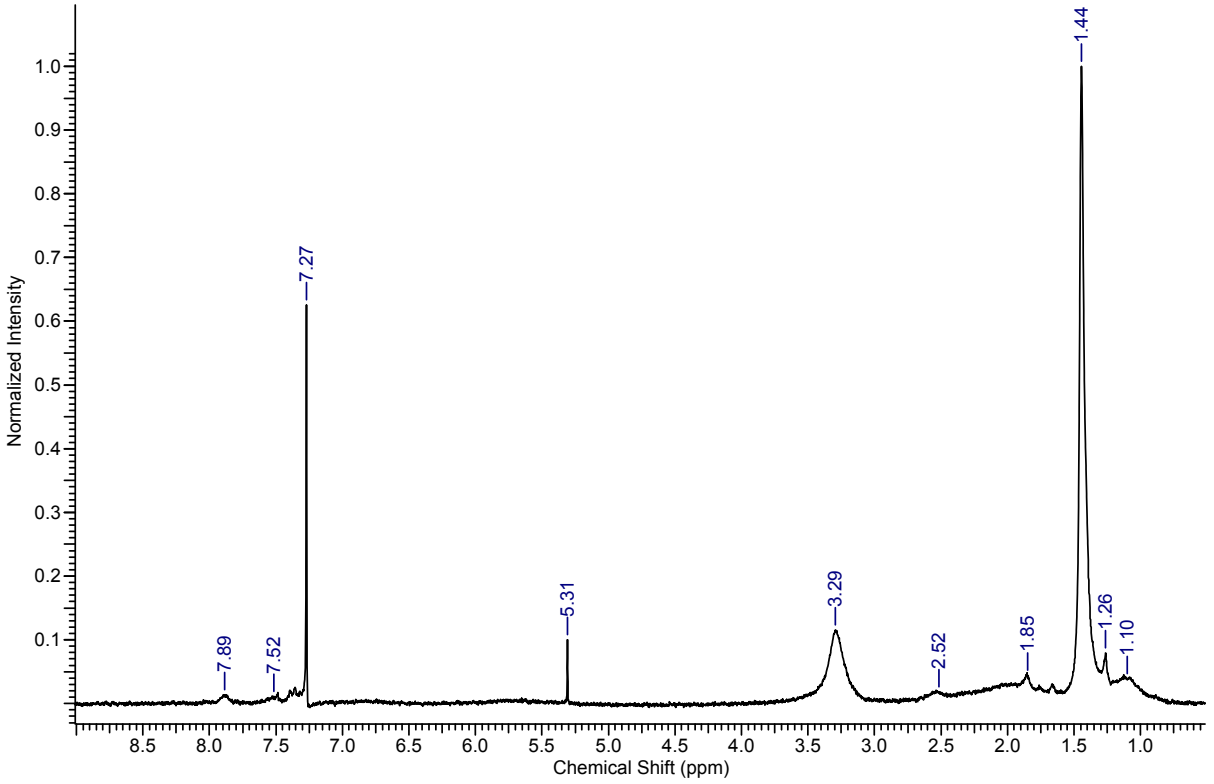

Figure S5. 200 MHz ^{1}H NMR spectrum of L3-Boc in $CDCl_3$

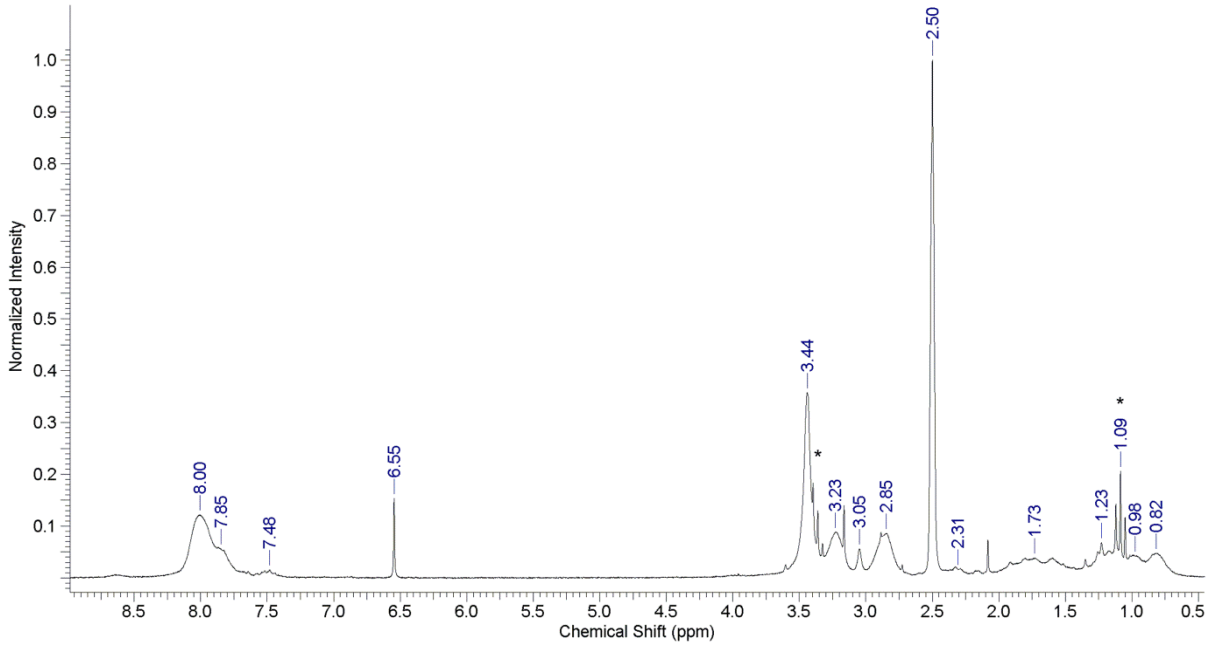

Figure S6. 200 MHz ^{1}H NMR spectrum of L3 in DMSO-d_6 (* Diethyl ether)

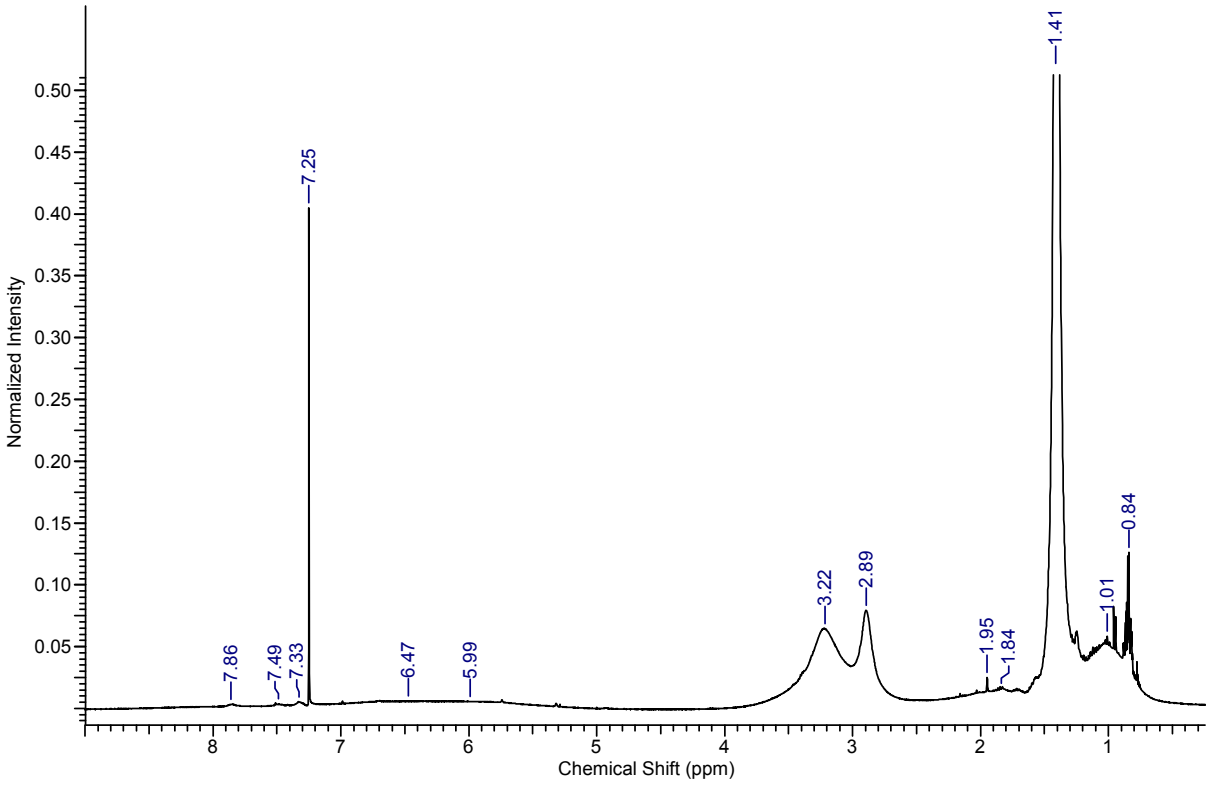

Figure S7. 400 MHz ^{1}H NMR spectrum of L4-Boc in $CDCl_3$

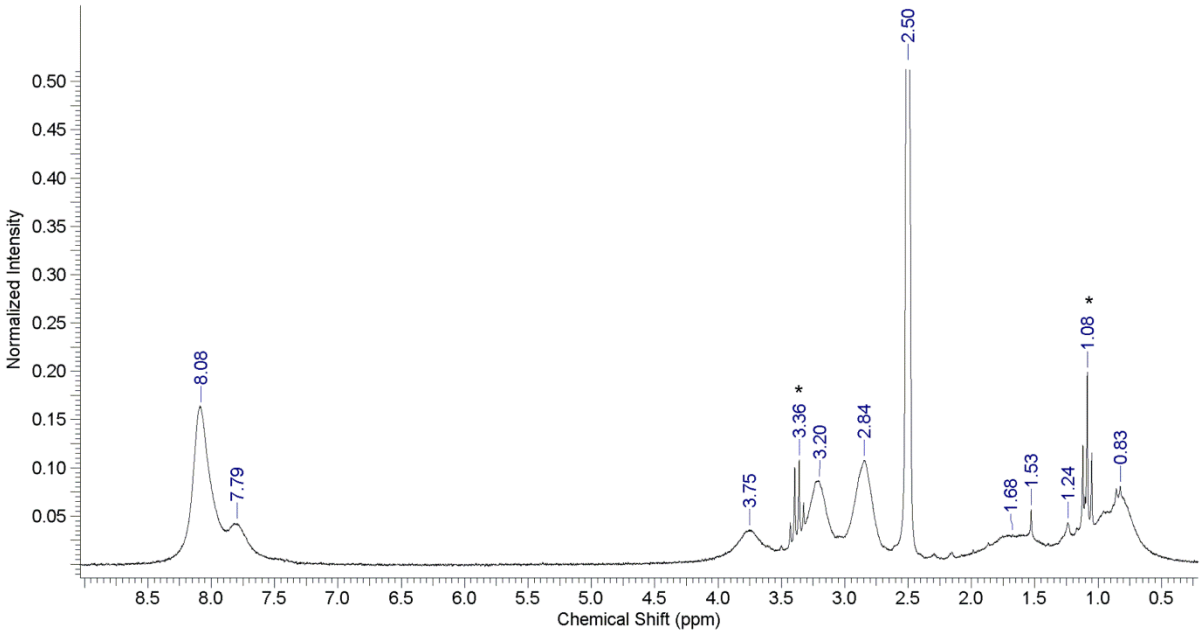

Figure S8. 200 MHz ^{1}H NMR spectrum of L4 in DMSO-d_6 (* Diethyl ether)

Section II

C) Experimental Section

Small angle X-ray scattering (SAXS) experimentswere performed on samples to identify their phase. All experiments were carried out on a Bruker Nanostar machine equippedwith a Cu rotating anode, with a tungsten filament (filament size 0.1*1mm). The SAXS was operated at a voltage of 45kVand current of 20mA.We used the characteristic Cu K_α radiation(wavelength = 1.54Å), and calibrated the detector with silver behenate. Samples were sandwiched between kapton films and pasted on a metallic holder with a hole for x-rays to pass through. Scattering data was collected on a multiwire gas filled Hi-star 2-D area detector and were reduced to 1-D using the Bruker offline software.

Rheological experiments were performed to determine the mechanical properties of these mesophases.Experiments were carried on the MCR 301 (Anton Paar) using a 8mm parallel plate assembly. Samples were carefully loaded on the plate after allowing several days for equilibration. All tests were carried out at 30^{o}C. Initially, we performed a stress ramp to determine the yield stress for the sample. We then loaded a fresh sample and conducted a creep test at a stress value significantly lower than the yield stress. The viscosity was calculated from the slope of the compliance curve. The yield stress, creep test parameters and viscosity are shown in Table ST1.

We performed optical microscopy between crossed polarizers on GMO/water/additive systems, to visualise their textures and identify phases. We used a Nikon Eclipse E600 POL with a conventional digital camera (Nikon) connected to a PC. Samples were mounted on a Linkam Shear cell CSS450 for controlled heating. The CSS450 stage is equipped with two heaters for the top and bottom plates. The sample was placed on the lower plate and sandwiched with a glass coverslip. The sample was heated at a rate of 5^{o}C/minute up to ~80^{o}C and was subsequently cooled to ambient temperature. We identify the H_{II} phase based on characteristic cone type textures and the L_α phase based on their streak-like textures. Polarized optical microscopy was used to assign the SAXS peaks to the H_{II} and L_α phases, since only a few peaks were observed for these phases. Fd3m and Ia3d phases are isotropic, and exhibit no texture under cross polarisation (SI Figure S10).

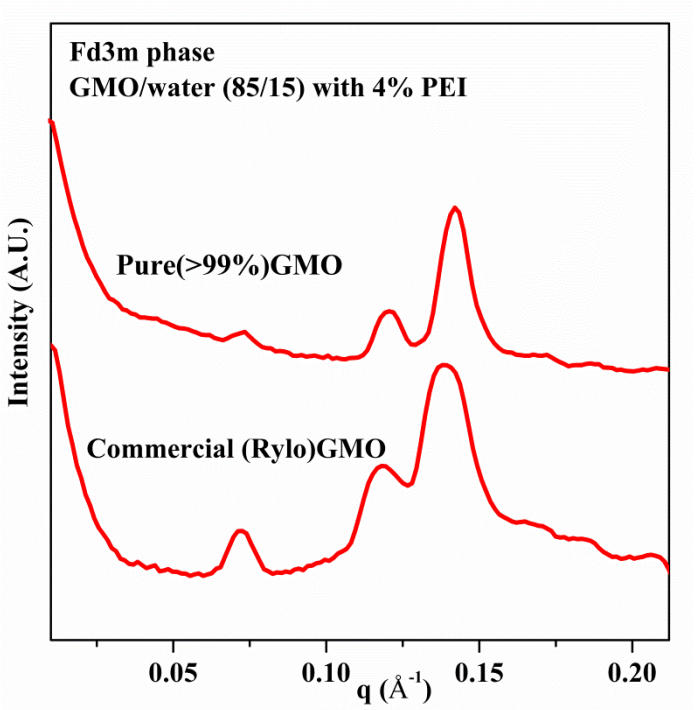

Figure S9: Control experiment comparing pure GMO (purity > 99%) and commercial GMO (Rylo) in ternary systems comprising GMO, water and a ternary polymeric additive (branched polyethyleneimine) in the ratio of 85:15:4, respectively.

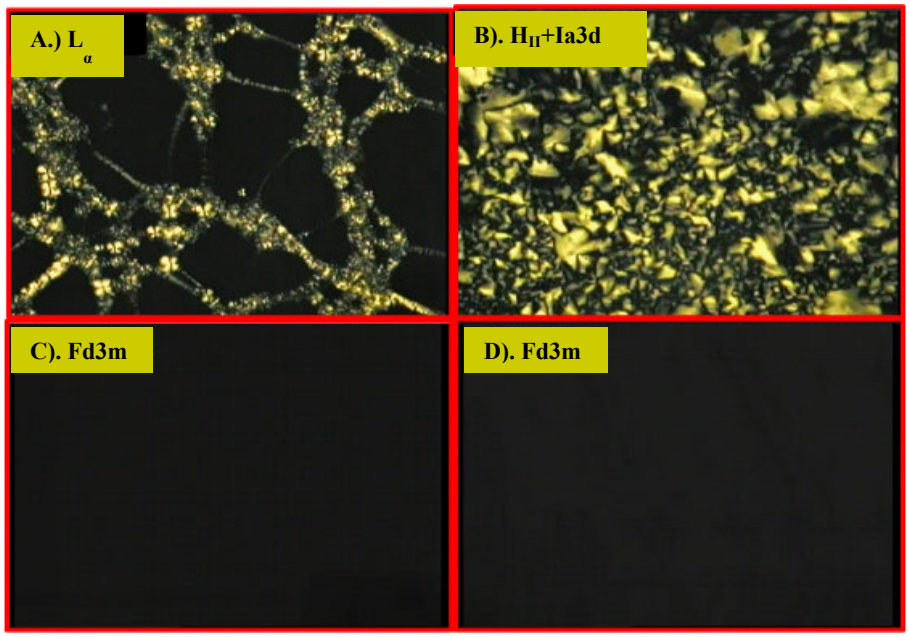

Figure S10: Optical images for different liquid crystalline mesophases between crossed polarizers. **A)** GMO/water/G4 (85/15/0) – streak like features characteristic of the Lα phase are observed; **B)** GMO/water/G4 (80/20/2) fan shaped structures characteristic of the H_{II}phase are observed; therefore, from the optical microscopy and SAXS, we can state that this composition corresponds to a coexistence of H_{II} and Ia3d phases; **C)** GMO/water/G4 (80/20/4); **D)** GMO/water/G4 (80/20/6). The Fd3m phases identified from SAXS for (C) and (D) are isotropic, and appear dark between crossed polarizers. These compositions (C and D) are turbid and are observed in the microscope as thin sample films.

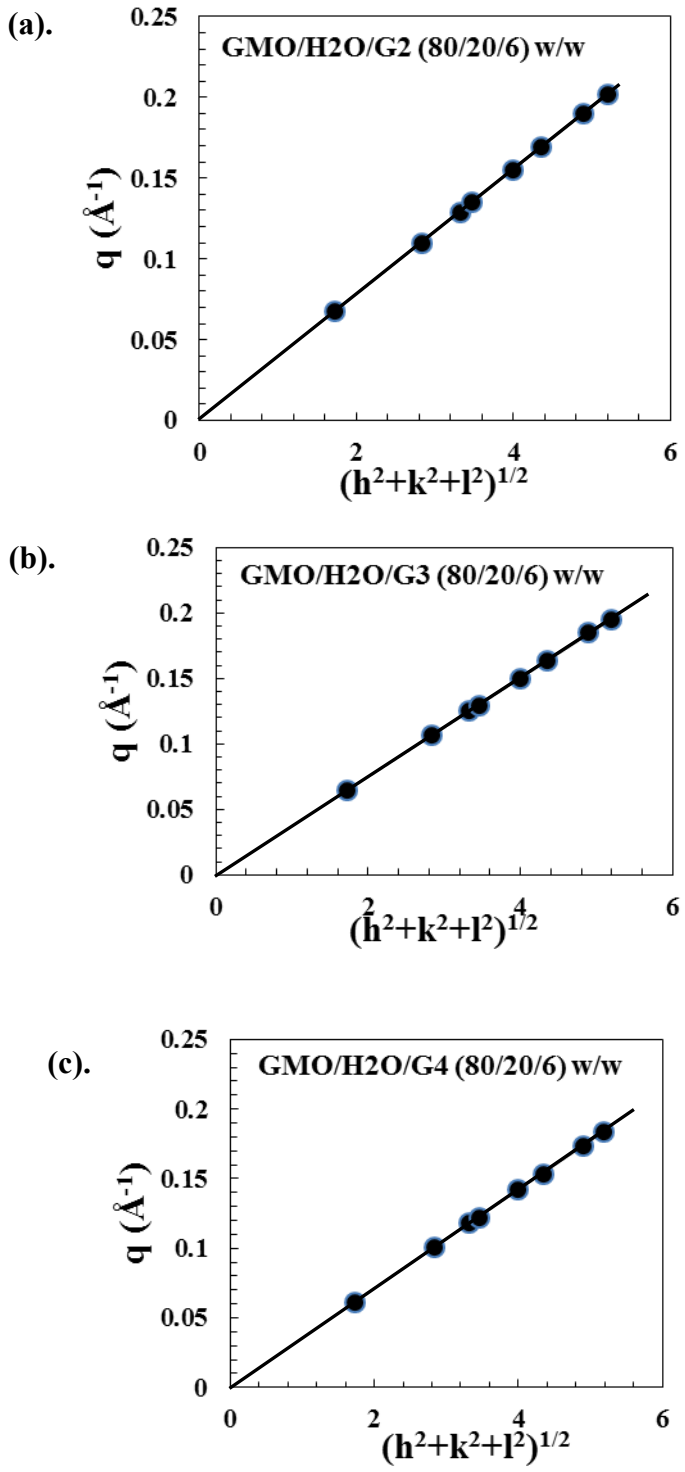

Figure S11: SAXS diffraction peaks for the GMO/water (80/20) w/w system in the presence of 6 wt. % G2, G3, and G4 are plotted as the peak spacing q_{hkl} *versus* $(h^2+k^2+l^2)^{1/2}$. The linear fit passes through the origin indicating that the system forms a structure with the Fd3m space group symmetry with lattice parameter **a)** 162±1 Å for G2 **b)** 166±2Å for G3 and, **c)** 173±1Å for G4.

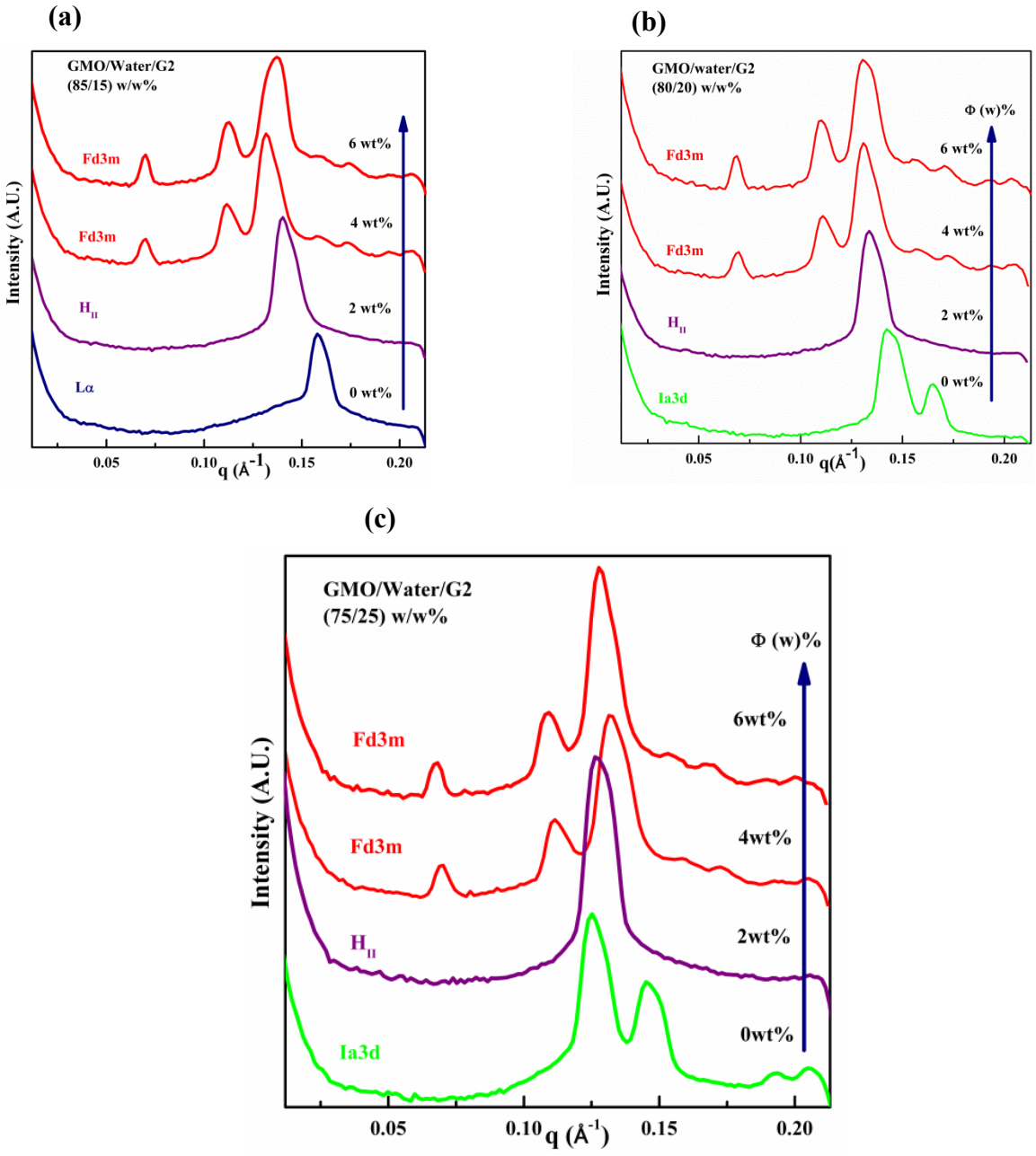

Figure S12: SAXS data for GMO/water**: (a)** 85/15 w/w; **(b)** 80/20 w/w; **(c)** 75/25 w/w containing Φ = 0, 2, 4 and 6 wt%, of G2 PAMAM dendron viz. the systems represent (a) 85/15/Φ; (b) 80/20/Φ and (c) 75/25/Φ.

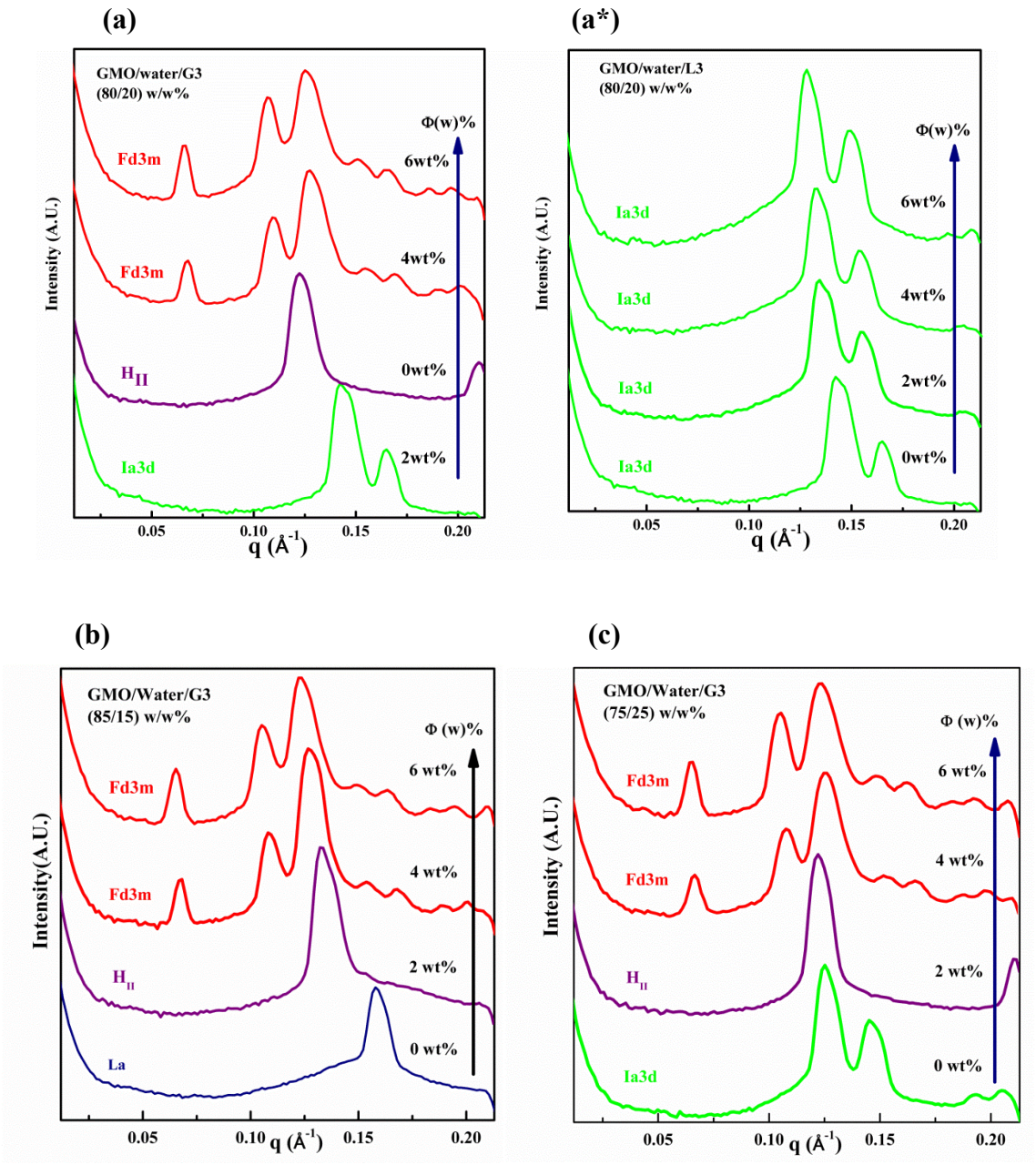

Figure S13: SAXS data for GMO/water**: (a)** and **(a*)** 80/20 w/w; **(b)** 85/15 w/w; **(c)** 75/25 w/w containing G3 PAMAM dendron and L3 (linear analog). The systems represent (a) 80/20/Φ_{G3}; (a*) 80/20/Φ_{L3} (b) 85/15/Φ_{G3} and (c) 75/25/Φ_{G3}, where Φrepresents the additive concentrations.

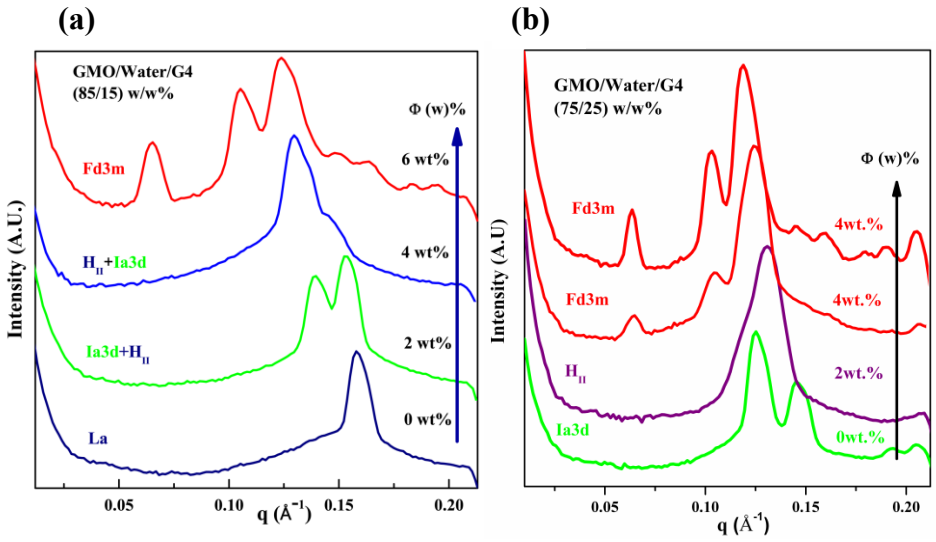

Figure S14: SAXS data for GMO/water**: (a)** 85/15 w/w; **(b)** 75/25 w/w containing Φ = 0, 2, 4 and 6 wt%, of G4 PAMAM dendron viz. the systems represent (a) 85/15/Φ and (b) 75/25/Φ.

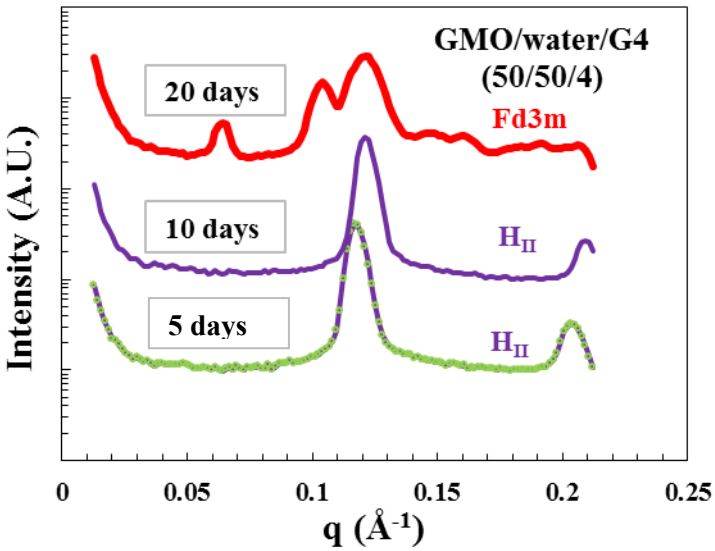

Figure S15: In a system containing GMO/water/G4 in the ratio 50/50/4, by weight, we observe a reverse hexagonal phase (peak ratio: 1:√3) at 5-10 days, that subsequently reorganizes to form an Fd3m phase that is observed after about 20 days of equilibration. Note that a cubic phase with Pn3m symmetry coexists with excess water for a binary 50:50 GMO/water system.

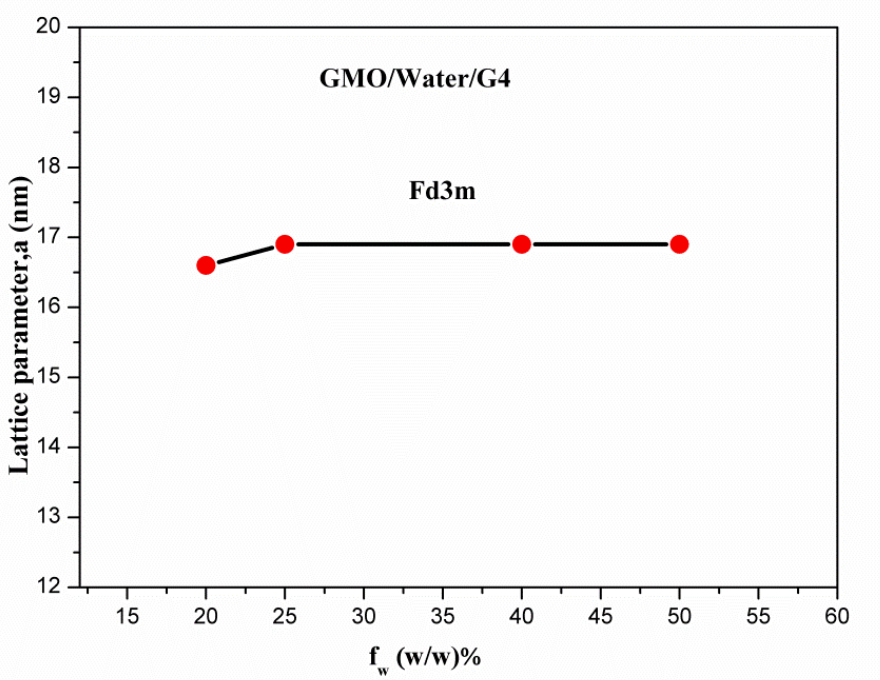

Figure S16: Lattice parameter for Fd3m phase in GMO/water/G4 PAMAM (Φ = 4%) system, as a function of water content.

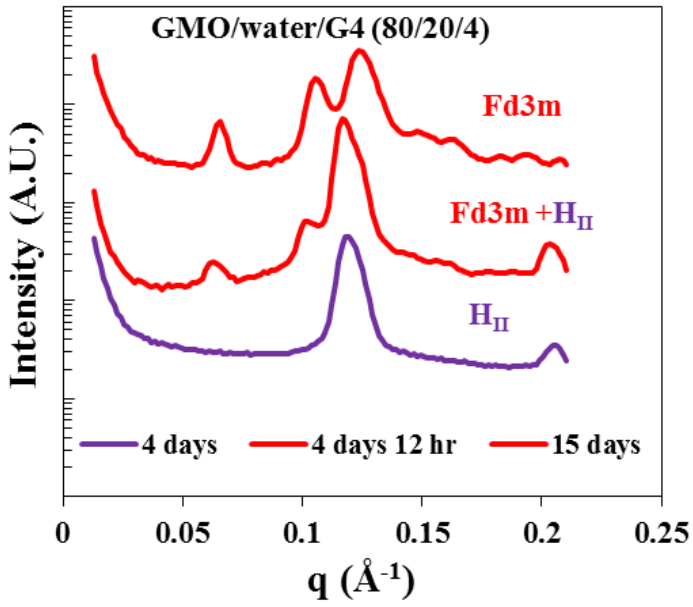

Figure S17: Kinetics of phase transformation: we observe structural changes for the 80:20:4 GMO/water/G4 systems as a function of equilibration time. This system forms the H_{II}phase in 4 days. We observe a coexistence of the H_{II} and Fd3m phases after about 4.5 days and finally, the Fd3m phase is observed after 15days of equilibration.

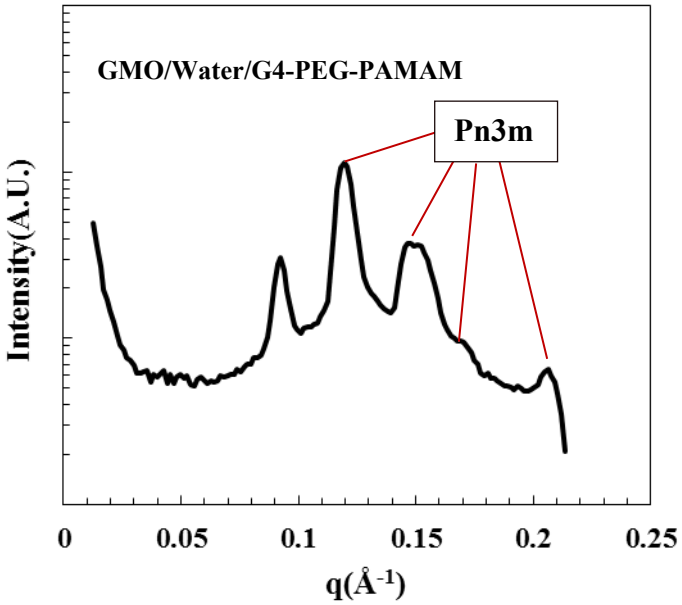

Figure S18: GMO/Water/PAMAM-G4-PEG system formed coexisting-Pn3m phase in 80:20:6 compositions (preferably Pn3m). Here, we modify the 1^{o} ammine at the surface of G4 dendron with 5-mer PEG-chains, and it transforms the Ia3d phase in GMO/water (80/20) system into Pn3m phase.

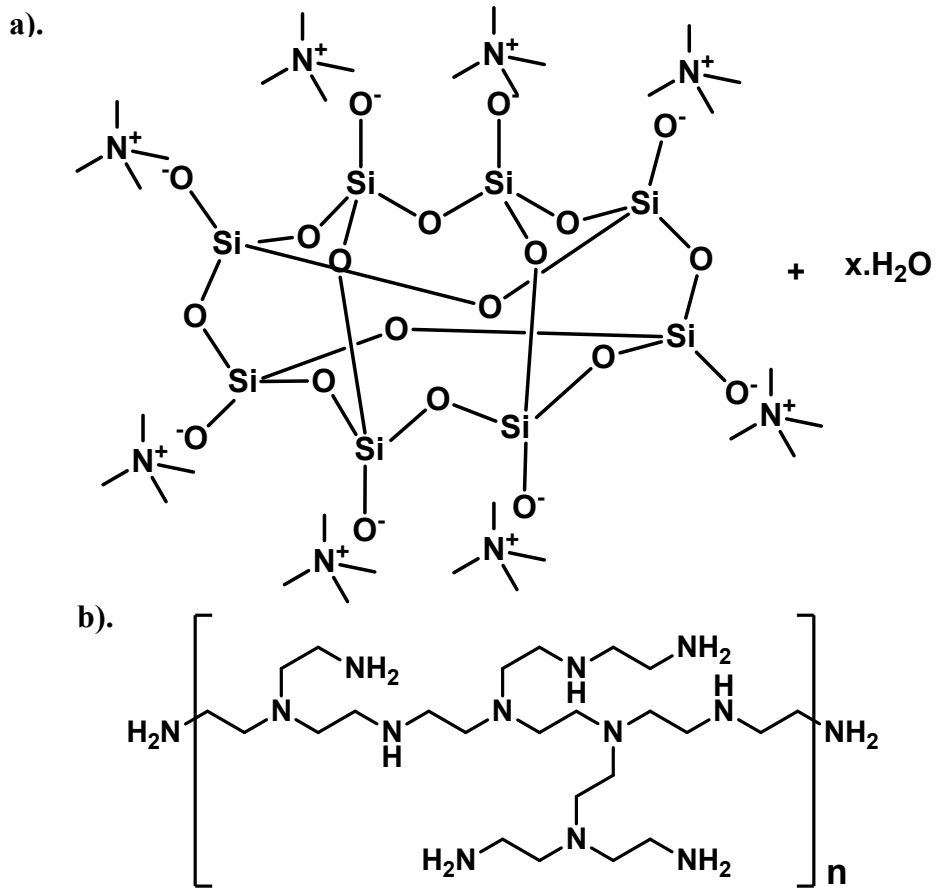

Figure 19. a) Represents the chemical structure for the POSS molecule b) Represents the chemical structure for branched PEI.

GMO/Water (80/20)						
CompositionStress rampStress for creep testViscosity						
(G4/L4)	**Yield stress (τ_y) Pa**		**Pa ($\tau < \tau_y$)**		**(η), Pa.s**	
Φ (w) %	**G4**	**L4**	**G4**	**L4**	**G4**	**L4**
0	2.36	2.36	0.8	0.8	10^4	10^4
2	28.9	------	9	-----	$2.5*10^4$	--------
4	45.6	36.3	9	9	$2*10^5$	$3.3*10^4$
6	68.4	11.7	9	9	$1.6*10^5$	$1.4*10^4$

Table ST1: Creep viscosity measurement for GMO/water (80/20) system with G4 and L4 as a function of Φ

GMO/water (85/15) w/w%			
Φ(w)%	G2	G3	G4
	a(Å)	a (Å)	a (Å)
0	39.8	39.8	39.8
2	52.0	54.8	…
4	156.0	162.7	…
6	159.3	166.2	169.9

Table ST2: Lattice parameter characterizing L_{α}, H_{II} and Fd3m phases for GMO/water (85/15) with G2, G3 and G4 PAMAM dendrons.

GMO/water (75/25) w/w%			
Φ(w)%	G2	G3	G4
	a(Å)	a (Å)	a (Å)
0	122.9	122.9	122.9
2	58.6	59.3	….
4	159.3	162.7	169.9
6	162.7	166.2	….

Table ST3: Lattice parameter characterizing Ia3d, H_{II} and Fd3m phases for GMO/water (75/25) with G2, G3 and G4 PAMAM dendrons.

Section III

Computational Analysis:

Distance Distribution Functions:

The trajectory of systems with 9 G4 molecules and 12 L-PAMAM molecules were visualized. From the snapshots (see Figure S22) we observe that G4 molecules assemble in water while L-PAMAM molecules do not form such aggregates. To understand this aggregation we have calculated radial distribution (see Figure S23a) of N- and O- atoms with other N- and O- atoms present in G4 and L-PAMAM. The peak heights for G4 molecule between 0.4 to 0.5 nm are higher than L-PAMAM which suggests interactions between G4 molecules are higher, which results in forming aggregates. When we consider the radial distribution of N-atoms with O atoms of G4 and L-PAMAM (see Figure S24b), we observe a dominant peak at 0.425 nm for G4. However, for L-PAMAM this peak is absent. These distributions consisted of intra- and intermolecular distances. There are three types of N-atoms present in a G4 molecule: (a) N-atoms of the *p*-amine moiety, (b) N-atoms of the amide group, and (c) N-atoms of the *t*-amine moiety. L-PAMAM molecule has N-atoms of the *p*-amines and N- atoms of the amide group. The *t*-amine moiety is absent for L-PAMAM molecule. We have also calculated the intramolecular distance distribution for *t*-amine N-atoms with O-atoms of the G4 (see inset of Figure S23b) which has a peak at 0.425. Thus, from the Figure S24b and its inset it is clear that the *t*-amine interactions in G4 which are absent for L-PAMAM, gives rise to the compactness. The inherent geometrical constraint in the G4 molecules also contributes to its compactness of each molecule.

The snapshots of the trajectory reveal that G4 molecules in GMO-water system are assembled together while the L-PAMAM molecules in GMO-water system are distributed over the bilayer (see Figure 6 of the main text). As G4 molecules form an aggregation, we further investigate to understand how the hydrophilic head groups of GMO interact with the G4 molecules. The snapshot suggests that the GMO bilayer curves to engulf the aggregated G4 molecules (see Figure 6 of the main text). Thus to analyze such interaction we have calculated the volume normalized distance distribution of the ether oxygen (O6, for the numbering of atom see Figure S20b) of GMO head group and N- and O- atoms of polymer in the interval of simulation time and plotted them in Figure S24a for G4 and S24b for L4. We find the peak at smaller distance (0.35 nm) increases as the simulation time is advanced. For L4 molecules, the shorter distance peaks are not found, the peak height is seen at a longer distance (beyond 0.50 nm). Thus this reflects that the G4 and GMO are coming closer as the curved-like structure is formed in the bilayer (see Figure 6 of the main text). While L-PAMAM molecules are distributed over the bilayer, they interact at a larger distance of 0.50 – 0.6 nm at the time intervals of 180-185 ns, 185-190 ns, and 190-195 ns and at 1.25 to 1.70 nm at 195-200 ns (see Figure S24b) and there are no sign of curvature in the bilayer (see Figure 6 of the main text).

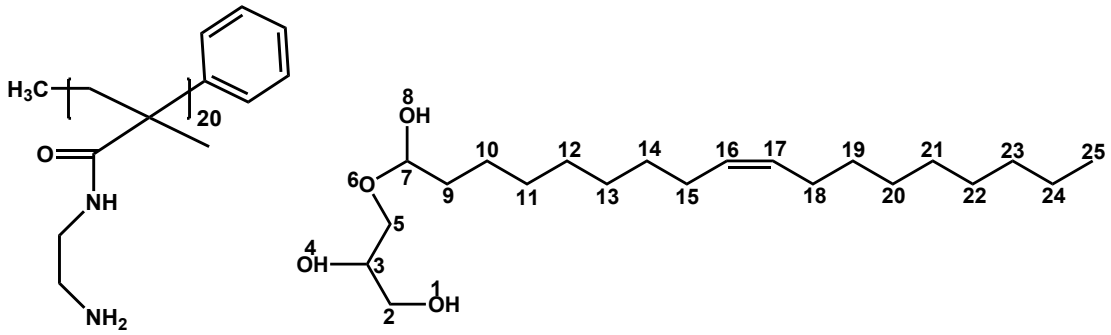

Figure S20: Structure of **(a)** modified L-PAMAM, and **(b)** GMO.

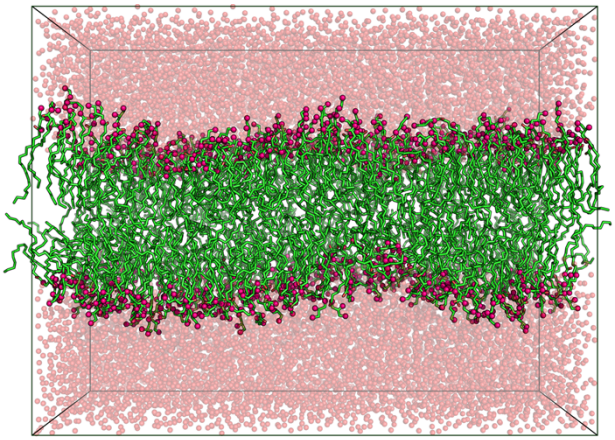

Figure S21: Representation of self-assembled GMO and water molecules. Water molecules are shown as spheres. H-atoms are not shown for clarity.

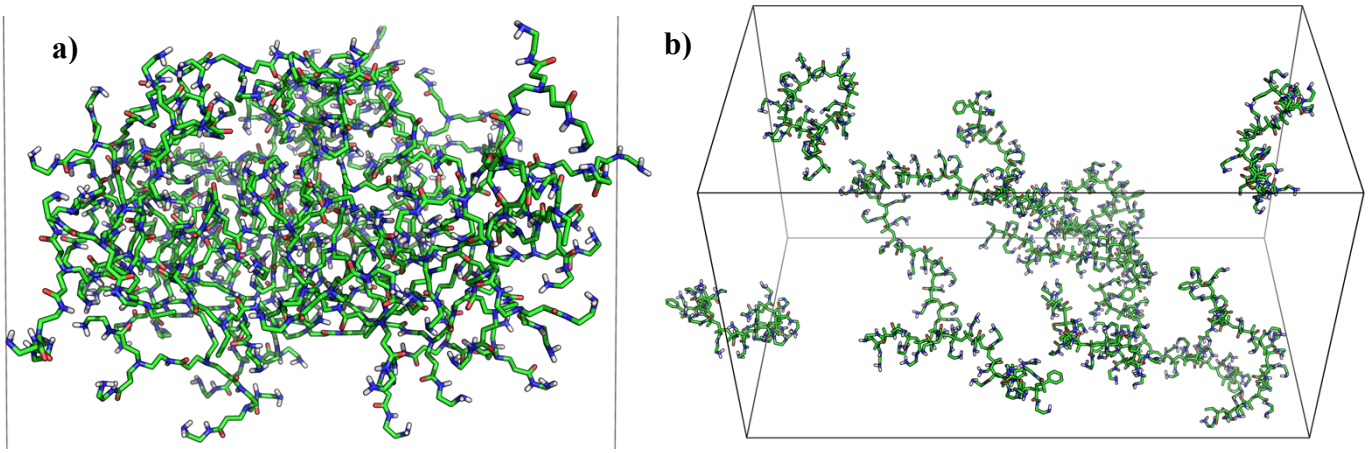

Figure S22:(a) Shows the collapsed state of G4. 9 G4 molecules form an aggregate. The aggregation is caused by the interaction of *t*-amine moiety and the amide -O- group. The geometrical constrained because of the model also play a role in aggregation. This snapshot corresponds to the 10^{th} ns of the simulation of G4 in water. **(b)** The L-PAMAM molecules are in extended state. The snapshot corresponds to the 10^{th} ns of the simulation of 12 L-PAMAM in water.

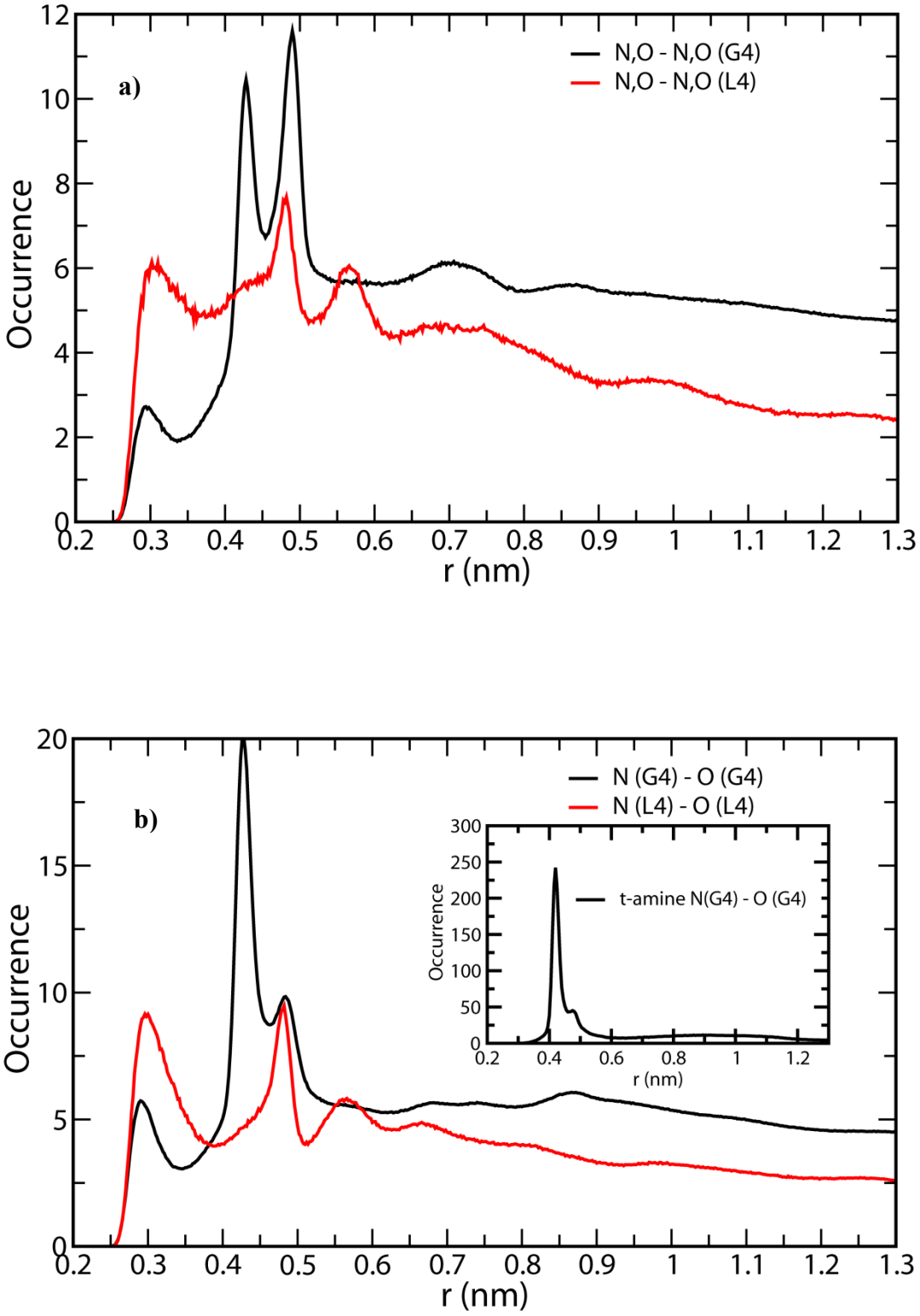

Figure S23: **(a)**The radial distribution of N, O atoms with other N, O atoms. **(b)** Shows the radial distribution of N atoms around the O atoms. In inset the intra-molecular volume normalized distance distribution between the *t*- amine moiety and the O atoms of G4 are plotted.

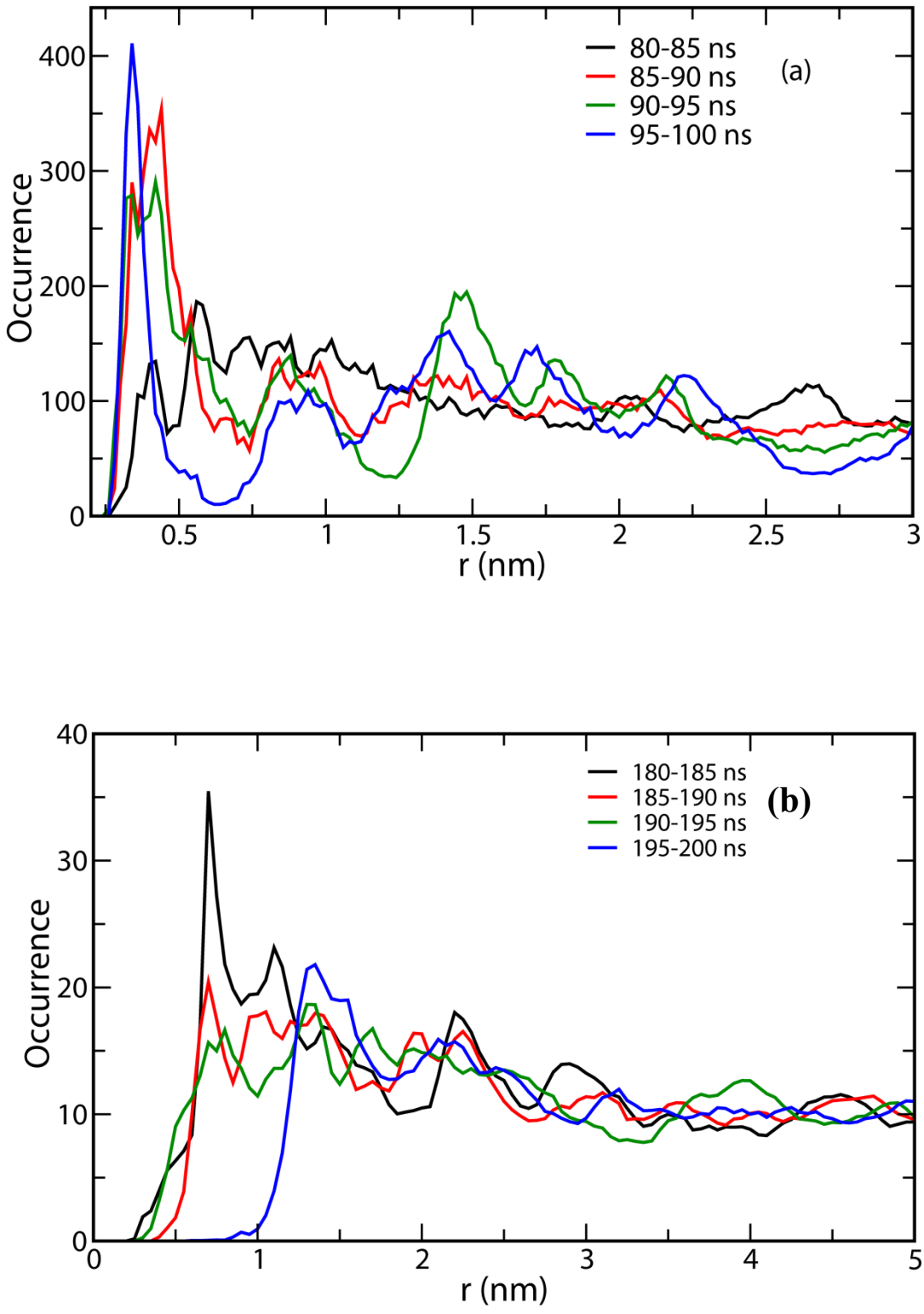

Figure S24: The volume normalized distance between the head group ether oxygen (O6) atom of GMO and the N and O atoms of the polymer, G4 (a) and L-PAMAM (b). We have computed the volume normalized distance distribution in the time intervals (mentioned in the legends). For G4 (a) the peak height at 0.35 nm increases with time while for the L-PAMAM (b) there is no prominence of such peaks.

Table ST4: Force Field Parameters for G4 (For structure refer Figure 2(5) of main manuscript). The molecule has been parameterized in four different parts (viz., terminal *p*-amines, *t*-amines, amidos, and acetylene moieties).

i) Acetylene Moiety

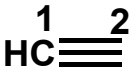

Atom	Opls type	Charge, *q*
C1	925	-0.210
H1	926	-0.200
C2	927	0.010

ii) t-amines Moiety

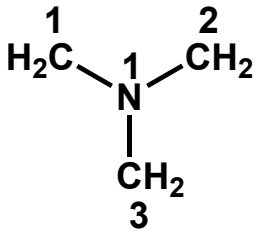

Atom	Opls type	Charge, *q*
C1, C2, C3	908	0.090
H11,H12, H21, H22, H31, H32	911	0.060
N1	902	-0.630

iii) Amido Moiety

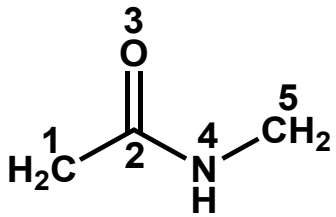

Atom	Opls type	Charge, *q*
C1	136	-0.120
C2	235	0.500
C5	244	0.080
H11, H12, H51, H52	140	0.060
O3	236	-0.500
N4	238	0.300
H4	241	0.080

iv) Terminal *p*-amines Moiety

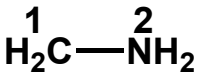

Atom	Opls type	Charge, *q*
C1	906	0.060
H11,H12	911	0.060
N2	900	-0.900
H21, H22	909	0.360

Table ST5: Force Field Parameters for L4 (For structure refer Figure S20(a) of SI). The molecule has been parameterized in three different parts (two terminal moieties and one repeating group).

v) Terminal Moiety

Atom	Opls type	Charge, *q*
C1	135	-0.18
H11, H12, H13	140	0.06

vi) Repeating Moiety

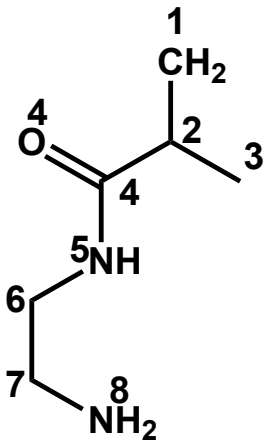

Atom	Opls type	Charge, *q*
C1, C3	135	-0.18
H11, H12, H31, H32, H33	140	0.06
C2	139	0.00
C4	235	0.5
O4	236	-0.5
N5	238	-0.5
H5	241	0.3
C6	244	0.08
H61, H62	140	0.06
C7	906	0.06
H71, H72	911	0.06
N8	900	-0.9

H81, H82	909	0.36

vii) Terminal Moiety

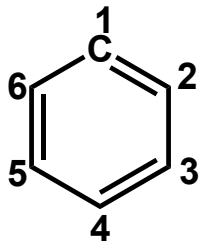

Atom	Opls type	Charge, *q*
C1	145	0.000
C2, C3, C4, C5, C6	145	-0.115
H21, H32, H41, H51, H61	146	0.115

Table ST6: In this work Lennard Jones parameter used forthe different atom types mentioned in Tables ST4 and ST5.

Opls type	σ (Å)	ε (kJ/mol)
135	0.350	0.276144
136	0.350	0.276144
139	0.350	0.276144
140	0.250	0.125520
145	0.355	0.317984
146	0.242	0.125520
235	0.375	0.439320
236	0.296	0.878640
238	0.325	0.711280
241	0.000	0.000000
244	0.350	0.276144
900	0.330	0.711280
902	0.330	0.711280
906	0.350	0.276144
908	0.350	0.276144
909	0.000	0.000000
911	0.250	0.062760
925	0.330	0.359824
926	0.242	0.062760
927	0.330	0.878640

References:

(1).C. V. Kulkarni, W.Wachter, G.Iglesias-Salto, S. Engelskirchen and S.Ahualli, *Phys. Chem. Chem. Phys.,*2011, **13**(8), 3004-3021.
(**2).** S. Deshpande,E. Venugopal, S. Ramagiri, J. R. Bellare, G. Kumaraswamy and N. Singh, *ACS Appl. Mater. Interfaces,* 2014, **6**(19), 17126-17133.